Applied Catalysis B: Environmental 160–161 (2014) 129–134

Contents lists available at ScienceDirect

Applied Catalysis B: Environmental

journal homepage: www.elsevier.com/locate/apcatb

The oxidation of trichloroethylene over different mixed oxides derived from hydrotalcites

Neus Blanch-Raga[a], A. Eduardo Palomares[a,*], Joaquín Martínez-Triguero[a], Marta Puche[a], Geolar Fetter[b], Pedro Bosch[c]

[a] Instituto de Tecnología Química, UPV-CSIC, Valencia 46022, Spain
[b] Facultad de Ciencias Químicas, BUAP, Puebla, PUE 72570, Mexico
[c] Instituto de Investigaciones en Materiales, UNAM, México D.F. 04510, Mexico

ARTICLE INFO

Article history:
Received 4 March 2014
Received in revised form 7 May 2014
Accepted 9 May 2014
Available online 16 May 2014

Keywords:
Catalytic oxidation
Trichloroethylene
Me^{2+}(Fe/Al) mixed oxides
Hydrotalcite-like compounds
Chlorinated VOCs

ABSTRACT

The activity of different Mg(Fe/Al), Ni(Fe/Al) and Co(Fe/Al) mixed oxides based on hydrotalcite-like compounds have been studied for the catalytic oxidation of trichloroethylene. It has been shown that the Co catalysts are more active than the Ni catalyst, being the Mg catalysts the less active ones. The activity of all the catalysts improves when iron is substituted by aluminum in the catalyst composition. The best results have been obtained with the CoAl mixed oxide derived from hydrotalcite that is a stable, highly active and selective catalyst. These results have been related with the presence of aluminum in the Co_3O_4 structure that favors, in the presence of oxygen, the formation of O_2^- sites and enhances the acid properties of the catalyst. The combination of both characteristics maximizes the adsorption and oxidation of the TCE.

1. Introduction

Chlorinated volatile organic compounds (CVOCs) are widely used in industry in different processes as petrochemical manufacture and dry cleaning. They are recognized as important air pollutants and their emissions contribute to the ozone layer destruction, to the photochemical smog and to undesirable human health effects. Trichloroethylene (TCE) is a common CVOC pollutant that is toxic, stable and probably carcinogenic to humans [1]. To control CVOC's emissions from stationary sources, thermal incineration is the most commonly used process, but it has important energetic costs because it operates at temperatures higher than 700 °C and chlorinated by-products can be formed. An interesting option to control CVOC emissions is the catalytic oxidation that makes feasible the operation at lower temperatures (250–550 °C) [2–4]. Metal oxides [5–8] or supported noble metals [9–11]. have been the most common catalysts used in this reaction, but they have some drawbacks as the poisoning by chlorine [4] and the formation of chlorinated by-products that can be very toxic [7,12]. Recently, other materials have been used for the catalytic oxidation of CVOCs as zeolites [13,14] and bronzes [15], but it is still necessary to find more active and stable catalysts. An alternative could be the use of mixed oxides derived from hydrotalcite-like compounds as catalysts for the CVOC oxidation.

Hydrotalcites are two-dimensional layered synthetic materials with alternating positively charged mixed metal hydroxide sheets and negatively charged interlayer anions [16]. By changing the nature and the molar ratio of the metal cations as well as the type of interlayer anions, many isostructural materials with different physicochemical properties can be obtained. The calcination of hydrotalcites leads to the formation of mixed oxides with interesting properties for the CVOC's catalytic removal, such as small particle size, large specific area and homogeneous interdispersion of the metals [17–20]. This work studies the use of mixed oxides derived from hydrotalcites, containing transition metals with oxidative properties, for the TCE catalytic oxidation reaction. The catalysts prepared are different Mg(Fe/Al), Ni(Fe/Al) and Co(Fe/Al) oxides based on hydrotalcite-like compounds and their activity have been compared with that of a H-MOR zeolite, which is a conventional catalyst used for this reaction [21]. The catalysts have been characterized by different techniques, *i.e.* gas adsorption (S_{BET}), X-ray diffraction (XRD), temperature-programmed desorption (NH_3-TPD), temperature-programmed reduction (H_2-TPR) and elemental analysis through inductively coupled plasma (ICP), in

* Corresponding author at: Instituto de Tecnología Química, UPV-CSIC, Campus de la Universitat Politècnica de València, Avda. Los Naranjos s/n, 46022 Valencia, Spain. Tel.: +34 96 387 78 06.
E-mail address: apalomar@iqn.upv.es (A.E. Palomares).

http://dx.doi.org/10.1016/j.apcatb.2014.05.014
0926-3373/

order to correlate their activity with the physical–chemical features of the materials.

2. Experimental

2.1. Catalysts preparation

The MgAl hydrotalcite was synthesized by mixing an aqueous solution (2.5 M) of $Mg(NO_3)_2{\cdot}6H_2O$ and $Al(NO_3)_3{\cdot}9H_2O$ with a 1.86 M solution of NaOH to obtain the desired Mg/Al molar ratio at a constant pH of 9. The resulting gel was treated in a microwave autoclave (MIC-I, Sistemas y Equipos de Vidrio S.A. de C.V.) for 10 min operating at 2.45 GHz with a microwave irradiation power of 200 W, while the temperature was maintained at 80 °C. The solid was recovered by decantation and washed several times with distilled water until the residual solution reached a pH value of about 8. Finally, the solid was dried at 60 °C for 24 h and calcined in air at 550 °C for 6 h.

NiAl, CoAl, MgFe, NiFe, CoFe, MgFeAl, NiFeAl and CoFeAl hydrotalcites were synthesized by using the simultaneous coprecipitation technique. An aqueous solution with the appropriate amounts of $Ni(NO_3)_2{\cdot}6H_2O$, $Co(NO_3)_2{\cdot}6H_2O$ or $MgCl_2$ and $FeCl_3$ or $Al(NO_3)_3{\cdot}9H_2O$ was mixed with a NaOH and Na_2CO_3 solution. Both solutions were added simultaneously with a flow rate of 60 mL h^{-1} at room temperature and atmospheric pressure and they were mixed under vigorous stirring. The resulting gel was dried overnight at 60 °C. The product was then filtered off and washed thoroughly with distilled water. The dried hydrotalcite was calcined in air at 550 °C for 6 h.

Zeolite NH_4-MOR (CBV 10AH with SiO_2/Al_2O_3 = 14 and surface area of 490 $m^2\ g^{-1}$) was supplied by Zeolyst Corp. and it was transformed into the H-form by calcination in air at 550 °C for 3 h.

2.2. Catalysts characterization

The chemical composition of the samples was measured by inductively coupled plasma (ICP-OES). Samples (*ca.* 20 mg), previously calcined, were dissolved in a HNO_3/HCl (1:3 vol.) solution and then analyzed in a Varian 715-ES ICP-Optical Emission Spectrometer.

BET surface areas were determined from the nitrogen adsorption–desorption curves by the conventional multipoint technique with a Micromeritics ASAP 2420. The samples were pretreated at 400 °C for 12 h at high vacuum.

A Phillips X'Pert diffractometer coupled to a copper anode X-ray tube was used for the XRD characterization, employing the K_α-Cu monochromatic radiation. Compounds were identified in the conventional way using the JCPDS file.

Temperature programmed reduction (TPR) experiments were carried out using a TPD-TPR Autochem 2910 analyzer equipped with a thermal conductivity detector (TCD). Samples (10–20 mg of catalyst) were treated with a N_2:H_2 flow (10% H_2) of 50 mL min^{-1} at a heating rate of 10 °C min^{-1} from room temperature to 800 °C.

Temperature programmed desorption of ammonia (TPD) experiments were carried out on a Micromeritics Autochem II analyzer, where 300 mg of sample were pre-treated in an Ar stream at 450 °C for 1 h. Ammonia was chemisorbed by pulses at 100 °C until equilibrium was reached. Then, the sample was fluxed with a He stream for 15 min, prior to increase the temperature up to 500 °C using a heating rate of 10 °C min^{-1}. The NH_3 desorption was monitored by both thermal conductivity detector (TCD) and mass-spectrometer, following the mass of ammonia at m/e = 15.

2.3. Catalysts activity

Catalytic oxidation reactions were carried out in a conventional quartz fixed bed reactor under atmospheric pressure. The catalysts were pelletized, and then crushed and sieved to obtain grains of 0.25–0.45 mm diameter. The catalyst bed (0.68 g) was supported on a quartz plug located into the reactor. Crushed quartz glass (>0.6 mm o.d.) was placed above the catalyst bed as a preheating zone of the incoming feed stream. The temperature was measured with a K-thermocouple located in the reactor, right before the catalyst bed. The reactor was housed in an electrically-heated furnace. Before reaction the calcined samples were activated at 150 °C with air during 30 min [15]. After activation, the gas mixture, composed by trichloroethylene (1000 ppm) and dry air, was introduced into the reactor at 400 mL min^{-1} (GHSV = 15,000 h^{-1}) and with a residence time of 0.24 s. The reaction was carried out under continuous flow of reactants, and each catalyst was tested at different temperatures, between 150 and 550 °C in steps of 50 °C keeping each temperature during 30 min. A blank experiment was made in the same reaction conditions but introducing only crushed quartz glass into the reactor without catalyst.

The reaction products (except Cl_2 and HCl) were separated, identified and quantified by a Bruker 450 gas chromatograph equipped with an HP-5 column. The concentration of TCE, as well as any other chlorinated hydrocarbon formed in the reaction was analyzed with a flame ionization detector, whilst the CO and CO_2 concentration was analyzed with a thermal conductivity detector. Analysis of both Cl_2 and HCl was performed by bubbling the effluent stream through a 0.125 M NaOH solution [22]. Cl_2 concentration was determined by titration with ferrous ammonium sulfate using *N*,*N*-diethyl-*p*-phenylenediamine as an indicator and the concentration of chloride ions in the solution was determined using an ion-selective electrode (Thermo Scientific, Orion Products).

3. Results and discussion

3.1. Catalysts characterization

Table 1 shows the specific surface area and the elemental composition of the calcined samples. The BET surface area of all samples varies between 80 and 255 $m^2\ g^{-1}$, obtaining the highest values with the Mg-containing catalysts, and the lowest with the samples containing cobalt. This is related with the higher crystallite size of the cobalt catalysts compared with the magnesium catalysts [23] (*e.g.* the crystallite size calculated from the Debye–Scherrer equation is 12 nm for CoAl and 4 nm for MgAl). In all the samples the partial replacement of iron by aluminum results in an increase of the surface area because the presence of aluminum diminishes the mean crystallite size of the samples [23] (*e.g.* the crystallite size calculated from the Debye–Scherrer equation is 19 nm for CoFe and 14 nm for CoFeAl).

The XRD patterns of the samples before and after calcination are displayed in Figs. 1 and 2. Before calcination (Fig. 1), all the samples present the characteristic diffraction peaks of a typical nitrated hydrotalcite [24–26] around 2θ = 10.9°, 22.2°, 34.2°, 38.7°, 44.7°, 60.1° and 61.2°, indicating that the hydrotalcite phase was successfully formed, independently of the preparation method and the nominal molar ratio. Nevertheless, the substitution of aluminum by iron in the hydrotalcite structure results in a modification of the peak broadening which can be attributed to a strain between the crystalline planes. Moreover the position of the peaks in the samples containing iron is shifted to lower values of 2θ degrees if compared with the samples with aluminum, due to the difference size of Fe^{3+} and Al^{3+} ions.

Table 1
Chemical composition and surface area of the catalysts.

Catalyst	S_{BET} ($m^2\ g^{-1}$)	Bulk composition of calcined samples (weight %)					Nominal molar ratio
		%Mg	%Ni	%Co	%Al	%Fe	
MgFe	189	25.7	–	–	–	17.2	Mg/Fe = 3:1
MgFeAl	252	26.4	–	–	6.6	4.1	Mg/Fe/Al = 3.75:0.25:0.75
MgAl	169	24.8	–	–	6.9	–	Mg/Al = 4:1
NiFe	143	–	40.1	–	–	19.2	Ni/Fe = 2:1
NiFeAl	218	–	46.0	–	4.8	3.6	Ni/Fe/Al = 3:0.25:0.75
NiAl	123	–	45.9	–	7.1	–	Ni/Al = 3:1
CoFe	81	–	–	45.9	–	14.7	Co/Fe = 3:1
CoFeAl	131	–	–	50.9	6.1	4.1	Co/Fe/Al = 3:0.25:0.75
CoAl	106	–	–	46.5	9.9	–	Co/Al = 2:1

After calcination, the hydrotalcites are converted into mixed oxides as it is reflected in the XRD pattern of the samples (Fig. 2). As it can be seen, the MgAl catalyst after calcination shows a periclase-like structure with the main characteristic peaks at $2\theta = 35.7°$, 43.3°, 62.8°, 75° and 79.4°. The NiAl catalyst presents the typical peaks associated to NiO at $2\theta = 37.4°$, 43.5°, 63°, 75.9° and 79.7°. The peaks of both catalysts are shifted to higher angles if compared with the pure oxide as consequence of the aluminum incorporation into the NiO or MgO framework [27], indicating the formation of a mixed oxide. On the other hand, the CoAl sample presents peaks at $2\theta = 31.3°$, 36.8°, 38.5°, 44.8°, 55.6°, 59.3°, 65.2°, 76.5° and 77.6°, which can be associated to Co_3O_4 (JCPDS 421467) and to other spinel phases as $CoAl_2O_4$ (JCPDS 440160) and Co_2AlO_4 (JCPDS 380814) as it is suggested by the shift of the peaks to higher angles if compared with a pure Co_3O_4 spinel [28]. On the contrary, the MgFe and NiFe samples show, together with the peaks of MgO or NiO, new peaks at 30.1°, 35.5°, 37°, 42.9°, 53.4°, 57.1°, 62.5°, 70.8°, 74.9° and 78.7°. These peaks are associated to a magnetite-like structure (Fe_3O_4) nevertheless they can also correspond to the formation of $MgFe_2O_4$ and $NiFe_2O_4$ spinel phases [29]. The CoFe sample presents the same peaks that the CoAl catalysts, which has been assigned to Co_3O_4. In this sample, there are no peaks that can be assigned Fe_3O_4, indicating that iron is incorporated in the structure of the spinel-like Co_3O_4 phase substituting some of the cobalt atoms. This is also suggested by the shift of the peaks assigned to Co_3O_4 to higher 2θ angles if compared with the peaks of a pure Co_3O_4 spinel.

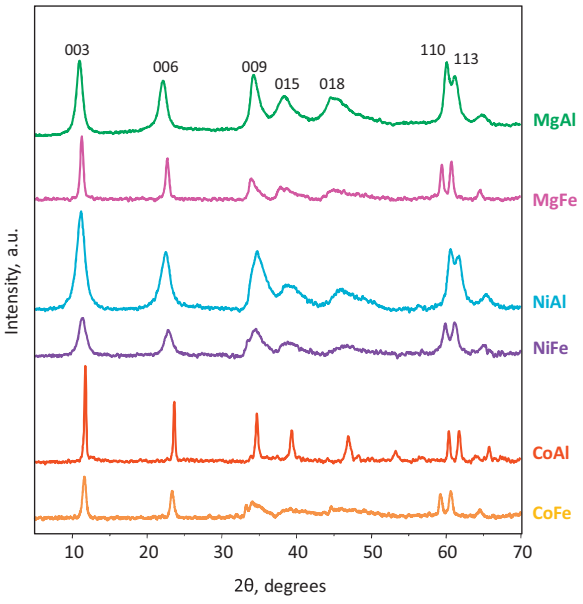

Fig. 1. XRD patterns of the samples before calcination.

The NH_3-TPD profiles of the Co- and Ni-containing samples are very similar for all the samples with a broad peak between 150 and 400 °C, being the main differences the quantity of ammonia adsorbed (Table 2). As the adsorption of NH_3 is related with the acidity of the material, it can be stated that the catalysts containing aluminum are more acidic than those with iron and that the catalysts with cobalt are more acidic than those containing nickel. In this way the CoAl sample is the more acidic one and the high quantity of ammonia adsorbed by this catalyst must be pointed out. This can be explained by the higher electronegativity of cobalt if compared with nickel [30] and, as it has been suggested from

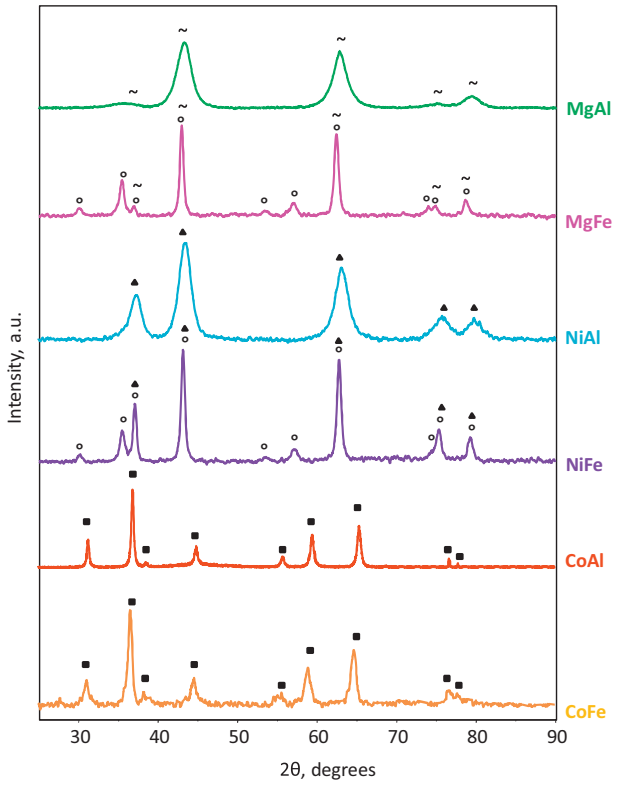

Fig. 2. XRD patterns of the samples after calcination (~ MgO, ▲ NiO, ○ Fe_3O_4, ■ Co_3O_4).

Table 2
NH_3-TPD results of the Ni- and Co-containing samples.

Catalyst	TPD results NH_3 adsorbed ($\mu mol_{NH_3}\ g^{-1}$)
NiFe	138
NiAl	349
CoFe	174
CoAl	539

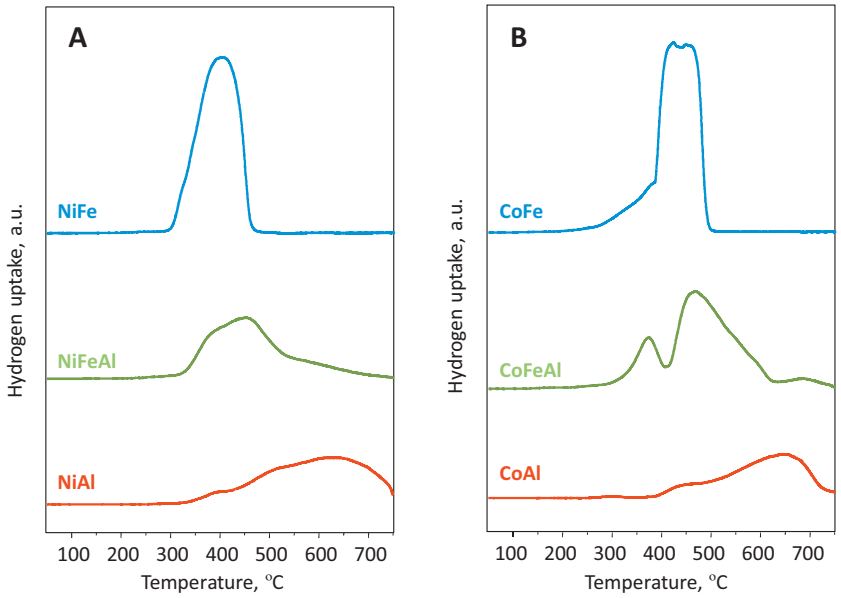

Fig. 3. TPR profiles of (A) Ni- and (B) Co-containing samples.

the XRD results, by the formation of a mixed oxide where the Al^{3+}—O—$Co^{3+/2+}$ bonds enhances the Lewis acidity of the Al^{3+}.

Temperature programmed reduction profiles obtained for the Ni- and Co-containing samples are shown in Fig. 3. It can be seen that the reduction peaks shift to higher temperatures when Fe is replaced by Al in the catalyst structure and that different profiles are displayed depending on the Al content. The NiFe sample (Fig. 3A) shows a high broad peak of hydrogen consumption between 300 and 450 °C. It matches with the reduction of NiO that typically features a broad single band located between 340 and 400 °C [31,32], but also with the reduction of Fe_3O_4, that occurs in the same temperature range [33,34]. When part of the Fe is replaced by Al (NiFeAl sample) this band reduces its intensity and shifts toward higher temperatures. The shift and the broadness of the bands are maximum with the NiAl catalyst, displaying a complex reduction pattern that indicates different and important interactions of nickel with aluminum [17] in this sample.

The TPR profiles of the Co-containing catalysts are shown in Fig. 3B. As it can be seen, the CoFe sample presents a high and broad peak between 400 and 500 °C with a small band between 275 and 400 °C. The highest reduction peak can be associated to the reduction of the spinel-like Co_3O_4 [23] and the lower band can be related to the reduction of the iron in the spinel [34]. As it occurred with the Ni-containing samples, when substituting Fe by Al (CoFeAl and CoAl samples) there is a shift of the main reduction peaks toward higher temperatures. In this way, the CoAl sample presents an undefined broad band between 400 and 700 °C that can be associated to the reduction of the cobalt atoms interacting with aluminum. It seems that the presence of aluminum hinders the reduction of the cobalt ions, probably because as it has been also suggested by the XRD and by the NH_3 TPD experiments, the Al^{3+} ions interacts with the Co-O bonds, polarizing them and increasing the effective charge of the Co ions [23,35] and therefore the reduction temperature [36].

3.2. Catalytic activity results

The catalytic activity for the oxidative decomposition of trichloroethylene was studied by the light-off curve, monitoring the conversion as a function of temperature for each catalyst. In Fig. 4 the catalytic activity of different Fe-catalysts was compared to the activity of the H-MOR zeolite, which has been described as an active catalyst for the TCE oxidation [21] and with a blank reaction. The catalytic activity of the zeolite started at 400 °C, the $T_{50\%}$ (temperature at which 50% conversion was reached) is 475 °C and the $T_{90\%}$ was higher than 550 °C. The results obtained with the MgFe mixed oxide ($T_{50\%}$ = 550 °C and $T_{90\%}$ > 550 °C) were much worse than those obtained with the reference catalyst and they were only slightly better than those of the blank reaction. The activity of the NiFe mixed oxide was similar to that of the zeolite catalyst ($T_{50\%}$ = 485 °C and $T_{90\%}$ = 550 °C) and the highest activity was achieved with the catalyst containing cobalt ($T_{50\%}$ = 395 °C and $T_{90\%}$ = 450 °C). This clearly indicates that the intrinsic catalytic activity of cobalt for the TCE oxidation is higher than that of nickel and magnesium.

The results obtained when there is a partial replacement of Fe by Al in the catalyst structure are shown in Fig. 5. Similarly to what occurred with the Fe-samples, the catalytic activity of the cobalt catalyst, CoFeAl, was the highest ($T_{50\%}$ = 350 °C and $T_{90\%}$ = 410 °C) and the catalytic activity of the magnesium catalyst, MgFeAl, was the lowest ($T_{50\%}$ = 540 °C and $T_{90\%}$ > 550 °C). The comparison of these

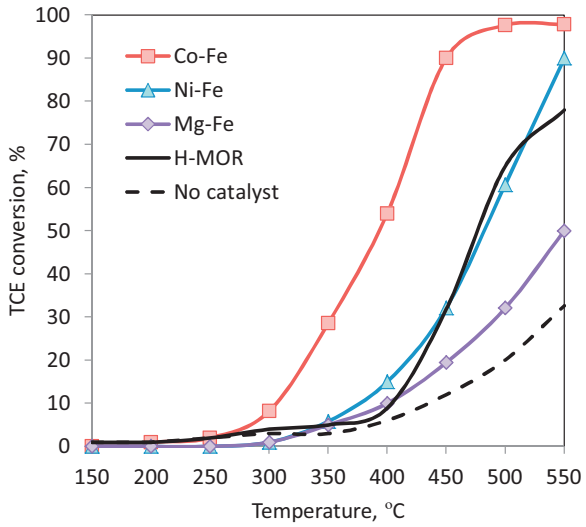

Fig. 4. TCE oxidation light-off curves over Fe-catalysts.

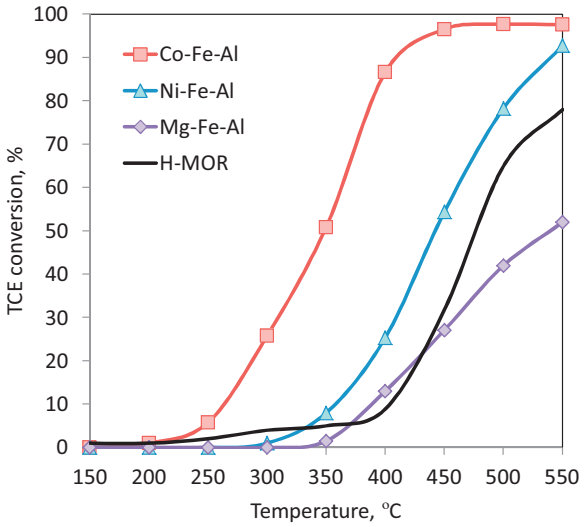

Fig. 5. TCE oxidation light-off curves over Fe/Al-catalysts.

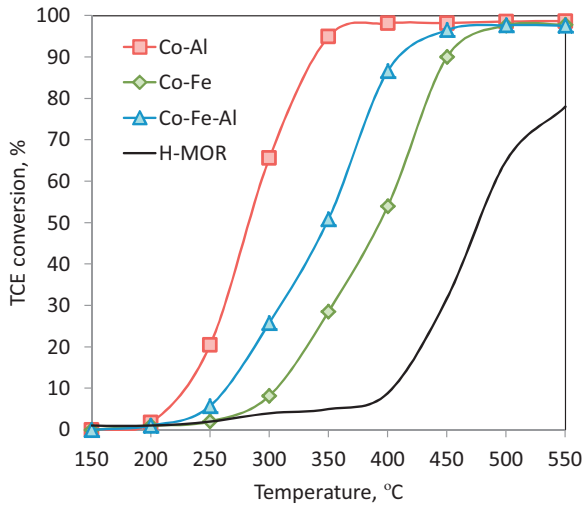

Fig. 7. TCE oxidation light-off curves over Co-catalysts.

results with those obtained with the Fe-catalysts (Fig. 4) clearly shows that the partial substitution of iron by aluminum results in a slight increase of the activity for all the catalysts tested. For that reason, a NiAl and a CoAl catalyst, without iron, were prepared and their activity for the TCE oxidation were compared with those of the NiFe(Al) and CoFe(Al) catalysts. The catalytic results for the Ni-containing samples are shown in Fig. 6. As it can be seen, although the $T_{90\%}$ for all the catalysts is the same, the reaction starts at lower temperature with the NiAl sample and an increase of the catalyst activity was observed as Fe was being substituted by Al ($T_{50\%}$ = 485 °C for NiFe, $T_{50\%}$ = 445 °C for NiFeAl and $T_{50\%}$ = 420 °C for NiAl). The same trend, but with better results, was observed for the Co-containing samples (Fig. 7) and the highest catalytic activity was achieved with the CoAl sample ($T_{50\%}$ = 280 °C and $T_{90\%}$ = 340 °C).

The enhancement of the catalytic activity for the TCE oxidation when substituting iron by aluminum in the catalyst structure is not related with the catalyst surface area, because the catalysts with the highest surface (the Fe/Al-samples) are not the most active ones. It seems that the activity of the catalyst must be related to the presence of aluminum in the catalyst framework and to the intrinsic activity of the other metals. It has been observed by H_2-TPR that the replacement of Fe by Al results in a strong interaction of the Al with the Co (or Ni), as it was evidenced by the shift of the TPR peaks to higher temperatures. This interaction polarizes the metal-O bonds, increasing the effective strength of the metal ions and then its acidity, as it was observed in the NH_3-TPD experiments. In addition, as it has been suggested when using this catalyst for other oxidation reactions [23], the surface of the Co–Al catalyst, in the presence of oxygen, is enriched in oxygen-ion-radicals that can oxidize the TCE adsorbed on the acid sites of the catalyst. According to previous works [23] an active assembly can be formed by the redox couple Co^{2+}/Co^{3+} and O_2^{x-} stabilized by the Al^{3+} ions that provide the TCE oxidation. The role of Al^{3+} ions in the generation of reactive superoxide species O_2^- has also been proposed by Wang et al. [37] for the CO oxidation using other materials and this is probably the reason for the increase of the catalyst activity when iron is substituted by aluminum in the catalyst structure.

Thus, the good results obtained with the CoAl catalyst can be explained by the high acidity of the material that favors the TCE adsorption and by the presence of reactive O_2^- species that oxidize the TCE.

Fig. 8 presents the product distribution of the TCE oxidation reaction when using the CoAl catalyst. The main oxidation products obtained were hydrogen chloride (HCl), chlorine (Cl_2) and carbon dioxide (CO_2). To a lesser extent tetrachloroethylene (C_2Cl_4)

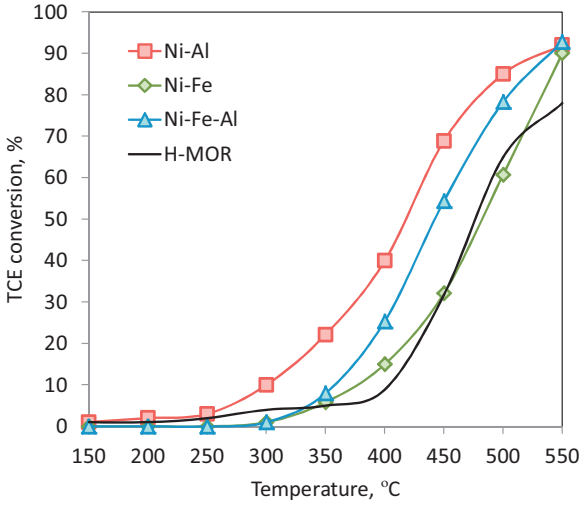

Fig. 6. TCE oxidation light-off curves over Ni-catalysts.

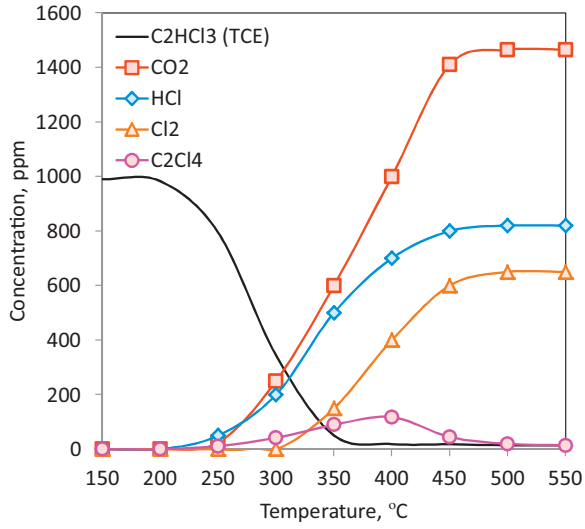

Fig. 8. Product distribution of TCE oxidation over the CoAl catalyst.

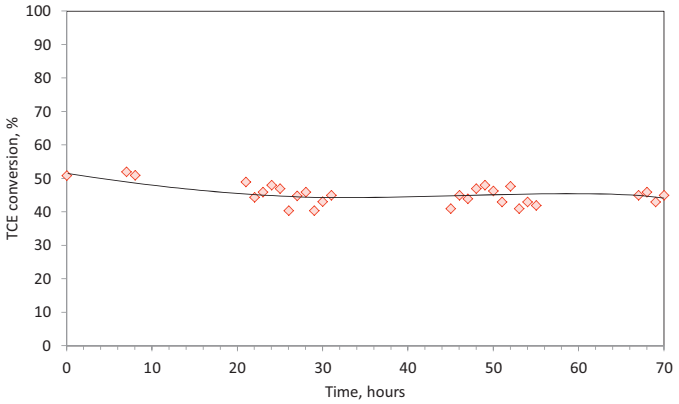

Fig. 9. TCE oxidation over the CoAl catalyst at 300 °C.

appeared, and traces of other chlorinated by-products, for example chloromethane, dichloromethane and carbon tetrachloride were found at mild temperatures in the product stream. It should be pointed out that no CO was detected at any temperature showing the good selectivity of the catalyst.

The catalyst stability was tested by doing a long term reaction at a constant temperature. The results obtained with the CoAl catalyst at 300 °C, temperature at which around 50% of TCE conversion was reached, are shown in Fig. 9. As it can be seen, the catalyst was stable at this temperature and there was not a significant deactivation after 70 h of reaction. These results indicate that Co-containing mixed oxides based on hydrotalcite-like compounds are highly active and stable catalysts for the TCE oxidation, being these results better than those obtained with an acid zeolite or with other type of catalysts based on bronzes or on Cu hydrotalcites [15,17].

4. Conclusions

Co(Fe/Al) mixed oxides based on hydrotalcite-like compounds present a high catalytic activity and selectivity for the oxidative decomposition of trichloroethylene. The catalysts containing aluminum are more active than those with iron probably because the presence of aluminum enhances the acid properties of the catalyst and generates reactive O_2^- species that oxidize the TCE. The CoAl sample is the most active catalyst ($T_{50\%}$ = 280 °C and $T_{90\%}$ = 340 °C), and its activity has been attributed to its higher acidity and to its oxidative properties. This catalyst is stable at 300 °C at least for 70 h of reaction.

Acknowledgements

The authors wish to thank financial support from CONACYT (project 154060) and from the Spanish Ministry of Economy and Competitiveness through the Consolider Ingenio Multicat (CSD-2009-00050) and MAT-2012-38567-C02-01 programms. N.B.R. acknowledges Cátedra Cemex Sostenibilidad (UPV) for a fellowship.

References

[1] J. Caldwell, R. Lunn, A. Ruder, IARC Monographs on the Evaluation of Carcinogenic Risks to Humans, 1995, pp. 75–158.
[2] J.N. Armor, Appl. Catal. B: Environ. 1 (1992) 221–256.
[3] Y.S. Matros, G.A. Bunimovich, S.E. Patterson, S.F. Meyer, Catal. Today 27 (1996) 307–313.
[4] J.J. Spivey, Ind. Eng. Chem. Res. 26 (1987) 2165–2180.
[5] S.K. Agarwal, J.J. Spivey, J.B. Butt, Appl. Catal. A: Gen. 82 (1992) 259–275.
[6] B. de Rivas, R. López-Fonseca, M.Á. Gutiérrez-Ortiz, J.I. Gutiérrez-Ortiz, Catal. Today 176 (2011) 470–473.
[7] A.M. Padilla, J. Corella, J.M. Toledo, Appl. Catal. B: Environ. 22 (1999) 107–121.
[8] G. Sinquin, J.P. Hindermann, C. Petit, A. Kiennemann, Catal. Today 54 (1999) 107–118.
[9] J.R. González-Velasco, A. Aranzabal, J.I. Gutierrez-Ortiz, R. Lopez-Fonseca, M.A. Gutierrez-Ortiz, Appl. Catal. B: Environ. 19 (1998) 189–197.
[10] R. López-Fonseca, J.I. Gutierrez-Ortiz, J.R. Gonzalez-Velasco, Appl. Catal. A: Gen. 271 (2004) 39–46.
[11] J.R. González-Velasco, A. Aranzabal, R. López-Fonseca, R. Ferret, J.A. González-Marcos, Appl. Catal. B: Environ. 24 (2000) 33–43.
[12] J.J. Spivey, J.B. Butt, Catal. Today 11 (1992) 465–500.
[13] H.L. Greene, D.S. Prakash, K.V. Athota, Appl. Catal. B: Environ. 7 (1996) 213–224.
[14] R. López-Fonseca, A. Aranzabal, J.I. Gutierrez-Ortiz, J.I. Alvarez-Uriarte, J.R. Gonzalez-Velasco, Appl. Catal. B: Environ. 30 (2001) 303–313.
[15] N. Blanch-Raga, M.D. Soriano, A.E. Palomares, P. Concepción, J. Martínez-Triguero, J.M.L. Nieto, Appl. Catal. B: Environ. 130–131 (2013) 36–43.
[16] A. Vaccari, Catal. Today 41 (1998) 53–71.
[17] N. Blanch-Raga, A.E. Palomares, J. Martínez-Triguero, G. Fetter, P. Bosch, Ind. Eng. Chem. Res. 52 (2013) 15772–15779.
[18] A.C. Camacho Rodrigues, C.A. Henriques, J.L. Fontes Monteiro, Mater. Res. 6 (2003) 563–568.
[19] A.L. McKenzie, C.T. Fishel, R.J. Davis, J. Catal. 138 (1992) 547–561.
[20] D. Tichit, M.H. Lhouty, A. Guida, B.H. Chiche, F. Figueras, A. Auroux, D. Bartalini, E. Garrone, J. Catal. 151 (1995) 50–59.
[21] R. Lopez-Fonseca, J.I. Gutierrez-Ortiz, M.A. Gutierrez-Ortiz, J.R. Gonzalez-Velasco, J. Catal. 209 (2002) 145–150.
[22] A.E. Greenberg, L.S. Clesceri, A.D. Eaton, Standard Methods for the Examination of Water and Wastewater, 18th ed., American Public Health Association, Washington, DC, 1992.
[23] M. Gabrovska, R. Edreva-Kardjieva, K. Tenchev, P. Tzvetkov, A. Spojakina, L. Petrov, Appl. Catal. A: Gen. 399 (2011) 242–251.
[24] A. Ayala, G. Fetter, E. Palomares, P. Bosch, Mater. Lett. 65 (2011) 1663–1665.
[25] E. Uzunova, D. Klissurski, I. Mitov, P. Stefanov, Chem. Mater. 5 (1993) 576–582.
[26] H.C.B. Hansen, C.B. Koch, R.M. Taylor, J. Solid State Chem. 113 (1994) 46–53.
[27] A.E. Palomares, J.G. Prato, F. Márquez, A. Corma, Appl. Catal. B: Environ. 41 (2003) 3–13.
[28] J. Pérez-Ramírez, G. Mul, F. Kapteijn, J.A. Moulijn, Mater. Res. Bull. 36 (2001) 1767–1775.
[29] M.S. Lee, J.Y. Lee, D.-W. Lee, D.J. Moon, K.-Y. Lee, Int. J. Hydrogen Energy 37 (2012) 11218–11226.
[30] A. Rodrigues, J. Math. Chem. 37 (2005) 347–351.
[31] M. Li, X. Wang, S. Li, S. Wang, X. Ma, Int. J. Hydrogen Energy 35 (2010) 6699–6708.
[32] K.V.R. Chary, P.V.R. Rao, V. Vishwanathan, Catal. Commun. 7 (2006) 974–978.
[33] W. Ramadan, M.I. Zaki, N.E. Fouad, G.A.H. Mekhemer, J. Magn. Magn. Mater. 355 (2014) 246–253.
[34] S. Song, H. Yang, R. Rao, H. Liu, A. Zhang, Appl. Catal. A: Gen. 375 (2010) 265–271.
[35] H.H. Kung, J. Catal. 73 (1982) 387–395.
[36] F. Al-Mashta, N. Sheppard, V. Lorenzelli, G. Busca, J. Chem. Soc., Faraday Trans. 1: Phys. Chem. Condens. Phases 78 (1982) 979–989.
[37] A. Wang, Y.-P. Hsieh, Y.-F. Chen, C.-Y. Mou, J. Catal. 237 (2006) 197–206.